Macromolecules

ARTICLE

pubs.acs.org/Macromolecules

Effect of Confinement on Structural Relaxation in Ultrathin Polymer Films Investigated by Local Dielectric Spectroscopy

Hung K. Nguyen,[†] Daniele Prevosto,[*,‡] Massimiliano Labardi,[‡] Simone Capaccioli,[†,‡] Mauro Lucchesi,[†,‡] and Pierangelo Rolla[†,‡]

[†]Dipartimento di Fisica "Enrico Fermi", Università di Pisa, Largo Pontecorvo 3, 56127 Pisa, Italy

[‡]Consiglio Nazionale delle Ricerche, Istituto per i Processi Chimico-Fisici, CNR-IPCF, c/o Dip. Fisica Largo Pontecorvo 3, 56127 Pisa, Italy

ABSTRACT: The effect of confinement on structural relaxation in ultrathin poly(vinyl acetate) films has been studied by local dielectric spectroscopy. This scanning probe method allows the investigation of dielectric relaxation at nanometer scale of supported ultrathin films having a free surface. Measurements have been performed at ambient pressure and controlled atmosphere on films with decreasing thickness. A deviation of dynamic properties from the bulk behavior, showing up as an increase of the relaxation rate, was observed starting from film thickness of 35 nm, which corresponds to about 3 times the gyration radius of polymer chains. A 2-fold increase of relaxation rate was measured for the thinnest investigated film of 18 nm. Local dielectric spectroscopy is therefore an effective method to elucidate confinement effects on relaxation dynamics in ultrathin polymer films with a free upper surface.

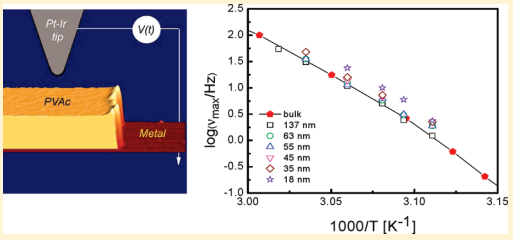

1. INTRODUCTION

In recent years, the understanding of confinement effects in dielectric relaxation studies of ultrathin polymer films can benefit from the removal of the upper metal electrode, which is customarily used for characterization by broadband dielectric spectroscopy (BDS), a technique of choice for the study of relaxation dynamics in polymers and glass-former materials. An example of drawbacks, eliminated thanks to the free upper surface, is represented by the interfacial effect due to penetration of metal atoms into the polymer film during the process of evaporation on the upper surface electrode that could affect dynamic behavior.[1,2] In order to determine how electrode deposition may affect BDS results, the so-called air-gap capacitor approach has been devised, consisting in a setup based on a partially filled capacitor, and has been used in previous studies,[3−5] where no change of dynamics in a variety of ultrathin polymer films with decreasing film thickness was detected. This appears in open contradiction with most of the evidence obtained on films capped on both sides[6−9] or even compared to the results by different techniques applicable to free-standing polymer films and with various geometrical arrangements.[10] Several other factors have been proposed to explain the observed discrepancy, such as the different physical quantities addressed by different techniques,[4] or the differences in preparative and experimental conditions.[5] However, alternate strategies to ascertain the role of interfacial interactions due to the deposited electrodes are demanded.

Electrostatic force microscopy (EFM)[11] and its numerous variants, which are based on the electrostatic interaction between a biased atomic force microscope (AFM) probe and a sample, have demonstrated their capability to study dielectric properties of materials with nanometer scale resolution.[12−21] In these techniques, one electrode is represented by the conductive substrate where the sample is deposited, and the second electrode is the conductive probe tip of the AFM itself. Most implementations until now have been exploited to measure dielectric constant of thin insulator films.[12−18] With a lateral resolution of tens of nanometers, obtained by using sharp tips, these techniques have been also applied to characterize dielectric properties of nanostructured materials where high spatial resolution is desired, such as polymer blends.[19]

More recently, local dielectric spectroscopy (LDS)[20,21] has been implemented to measure dynamic relaxation in insulator films with a free surface. LDS could therefore be proposed to investigate confinement effects in ultrathin polymer films having a free upper surface. A further advantage of this technique is the possibility to measure dielectric behavior of a small volume of material, releasing the need of continuous and uniform ultrathin polymer films to avoid short circuits between the substrate and the upper electrode.

LDS was first applied to characterize the complex dielectric permittivity of poly(vinyl acetate) (PVAc) films of thickness ~1 μm under ultrahigh-vacuum conditions.[20] The results showed a reduction in T_g of 4 K, and a narrowed distribution of relaxation times, attributed to the predominant contribution to the EFM signal of a thin free-surface layer (about 20 nm) of the film. In a previous work, we used this technique to study the influence of inorganic nanometric inclusions on relaxation dynamics of ultrathin PVAc films at ambient pressure. A slowing down of

Received: February 24, 2011
Revised: July 11, 2011
Published: July 28, 2011

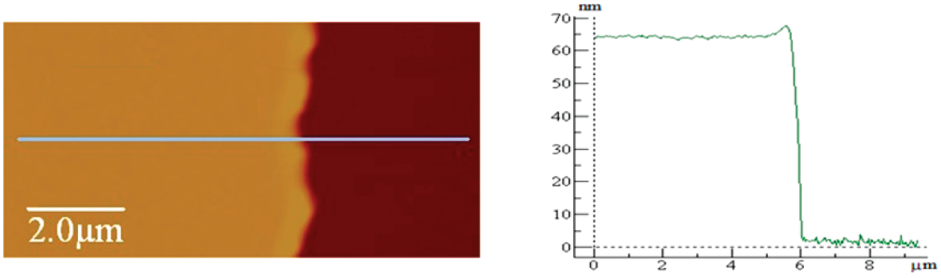

Figure 1. AFM topography map (left) of a thin polymer film with a scratch and line profile (right) that allows to measure film thickness.

structural dynamics at the interfacial regions between PVAc and silicate nanoparticles was detected.[21] In the present study, we apply LDS at ambient pressure and controlled humidity to address the effect of confinement on dynamic relaxation of ultrathin PVAc films. By choosing the latter material, we are able to compare our results with previous investigations performed using a number of different techniques and geometries.

2. EXPERIMENTAL METHODS

2.1. Sample Preparation. Poly(vinyl acetate) (PVAc) with molecular weight M_w = 167 000 g/mol and gyration radius R_g ~12 nm was purchased from Sigma-Aldrich. Ultrathin PVAc films were prepared by spin-coating solutions of PVAc in toluene onto gold substrates. Gold layers of 30 nm thickness were obtained by thermal evaporation on a glass disk previously evaporated with a ~5 nm adhesion layer of chromium. The PVAc thickness was controlled by changing the concentration of polymer solutions as well as spinning speed. PVAc films with thickness ranging from 18 to 140 nm were prepared and characterized in this study.

Prior to dielectric measurements, polymer films were annealed at about 10 K above the glass transition temperature under vacuum for at least 2 days. The measurement and annealing procedure was repeated several times to verify that the solvent was completely removed from the sample by checking the reproducibility of measured spectra. Before measurements, a scratch was made on the films by a steel cutter in order to uncover part of the metal electrode beneath. AFM profiling of the scratch was also used to determine the film thickness of our samples, as shown in Figure 1.

2.2. LDS Method and Data Analysis. In LDS operation, an excitation voltage, $V(t)$, is applied to the conductive tip of an AFM, which is positioned at a nanometric distance from the sample surface. The originating electric field induces a polarization in the sample region close to the probe. The force field due to interaction of the charged probe with the polarized sample induces a variation of the cantilever resonant frequency, Δf, which at the first order is due to the z-gradient of the electrostatic force F_{el}, between the tip apex and the sample:

$$\frac{\Delta f}{f_{res}} = -\frac{1}{2k}\frac{\partial F_{el}}{\partial z} \tag{1}$$

where k and f_{res} are the spring constant and the free resonant frequency of the AFM probe, respectively, and z is the tip−sample distance. The resonant frequency shift can be measured by operating the EFM in frequency-modulation (FM) mode.[22]

To describe F_{el}, the expression used in most of the EFM literature is

$$F_{el} = \frac{1}{2}\frac{\partial C}{\partial z}\Delta V^2 \tag{2}$$

with C the capacitance of the tip/sample system and ΔV their potential difference. It should be pointed out that eq 2 holds only for cases in which the tip apex−sample distance is smaller than the characteristic sizes of the probe, as in our investigation, and when one of the electrodes is grounded. The tip/sample capacitance can be expressed by an approximated relation working adequately in the distance range (of the order of the radius of the probe apex, R) where the present measurements have been performed[16]

$$C(z) = 2\pi\varepsilon_0 R \ln\left\{1 + \frac{R(1-\sin\theta)}{z + h/\varepsilon}\right\} \tag{3}$$

where h and ε are the thickness and the relative dielectric permittivity of the sample, respectively, θ is a parameter describing the aperture half-angle of the probe shaft, assumed of conical shape, and ε_0 is the permittivity of vacuum.

The variation $\Delta f(t)$ induced by the applied harmonic voltage $V(t) = V_0\cos(\omega t)$ and the contact potential difference presents three main terms: a dc shift, a term at the same frequency of the modulation bias, $\Delta f_\omega(t)$, and a term at its second harmonic, $\Delta f_{2\omega}(t)$.[23] To measure dielectric permittivity, the latter term is used since it is only influenced by capacitive interactions, while both the dc and first harmonic ones are also affected by the contact potentials between the tip and the sample.[24] To describe the dielectric relaxation of polymer films, the complex dielectric function $\varepsilon(\omega) = \varepsilon'(\omega) - i\varepsilon''(\omega)$ can be used. Then, the capacitance is also described itself as a complex function: $C(\omega) = C'(\omega) - iC''(\omega)$. By combining eqs 1 and 2, $\Delta f_{2\omega}(t)$ can be expressed as a function of the complex capacitance as

$$\Delta f_{2\omega}(t) = R\mathrm{e}\left[-\frac{f_{res}}{4k}V_0{}^2\frac{\partial^2 C}{\partial z^2}\mathrm{e}^{i2\omega t}\right] \tag{4}$$

The presence of an imaginary part of the system capacitance reflects the existence of a phase lag, in the following also called loss angle, δ_v, of $\Delta f_{2\omega}(t)$ with respect to the excitation voltage, originating from the dielectric loss mechanism. Equation 4 can be rewritten as

$$\Delta f_{2\omega}(t) = \Delta f^0_{2\omega}\cos(2\omega t - \delta_v) \tag{5}$$

with

$$\tan\delta_v = \frac{\partial^2 C''/\partial z^2}{\partial^2 C'/\partial z^2} \tag{6}$$

$$\Delta f^0_{2\omega} = -\frac{f_{res}}{4k}V_0{}^2\sqrt{\left(\frac{\partial^2 C'}{\partial z^2}\right)^2 + \left(\frac{\partial^2 C''}{\partial z^2}\right)^2} \tag{7}$$

A detailed description of the LDS method can be found in the literature.[20,21] A brief sketch of our experimental implementation is given in the following. In order to perform dielectric measurements, we used a double-pass technique, in which we disable the lateral scanning and the tip is maintained at a fixed location. During the first pass, the sample is approached with the usual tapping-mode operation. During the second pass, the tip is lifted by a constant height, and at the same time, the excitation bias is applied by using an automatic switch. The variation of $\Delta f_{2\omega}(t)$ is detected in both amplitude and phase shift, δ_v, using a dual-phase lock-in amplifier. Measurements within a range of frequencies (in our study, between 1 and 100 Hz) form a local dielectric spectrum.

dx.doi.org/10.1021/ma200440z |*Macromolecules* 2011, 44, 6588–6593

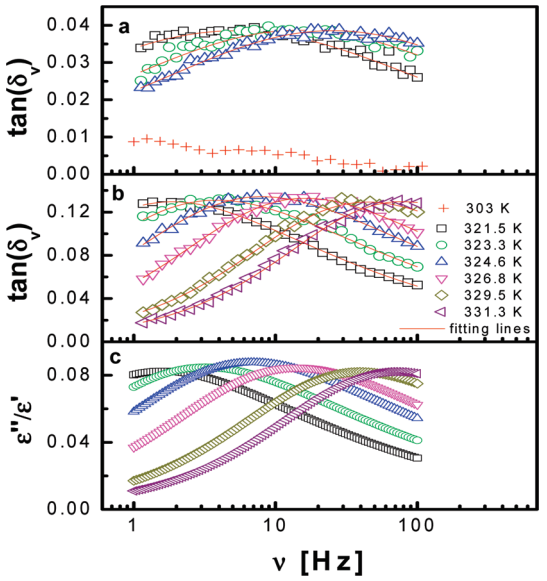

Figure 2. Phase shift tan δ_ν spectra (symbols) with fitting lines obtained by eqs 3, 6, and 8 on films of thickness 18 nm (a) and 137 nm (b). Dielectric tan $\delta = \varepsilon''/\varepsilon'$ spectra obtained from the fitting parameters (eq 8) as a function of frequency at different temperatures (film thickness 137 nm) (c).

Each of our loss-tangent spectra must be referred to a calibration (baseline) measurement obtained on the bare-metallic substrate to take into account and subtract all instrumental contributions to the signal. For calibration, the tip is positioned on the region of the scratch where the metal electrode is uncovered and a dielectric spectrum similar to the ones measured on the polymer film is recorded. This calibration is repeated at each temperature and is performed by keeping the same distance between the tip and the metal substrate as that while the tip was located on the polymer region. This ensures to keep the same geometric arrangement between film and calibration measurements.

In this work, a Veeco Multimode AFM was used (Nanoscope IIIa with ADC5 extension) operated in lift mode. FM-EFM was implemented through an electronics extender module (Quadrex), while signal access for external processing was obtained through a signal access module (SAMIII). For electric excitation and acquisition of dielectric spectra, an external dual-phase lock-in amplifier (SRS SR830DSP) controlled through General Purpose Interface Bus (GPIB) by a home-made LabView routine was used. Doped silicon (Nanosensors PPP-FMR) AFM cantilevers were used, with spring constant $k \sim 3$ N/m, resonant frequency $f_{res} \sim 70$ kHz, and guaranteed tip radius of less than 30 nm. Oscillation amplitude was calibrated as customary by AFM tapping mode amplitude/distance curves. By this way, the distance between the AFM tip and the sample surface during the electric measurements was calculated by summing the average tip−sample distance on tapping mode with the set-lift height. For all dielectric measurements, the tip/sample distance was estimated around 20 nm.

Our microscope was operated in controlled atmosphere within a home-made enclosure that allows keeping relative humidity as small as 3% (typical value less than 8% for all reported measurements). The sample temperature was controlled using a thermal application controller (TAC, Veeco). The actual temperature on the sample surface was checked by a remote thermometry method[25] using a fluoroptic thermometer (Luxtron 710).

3. RESULTS AND DISCUSSION

Phase shift spectra δ_ν were measured on each polymer film at different temperatures. The tangent of δ_ν for films with thickness

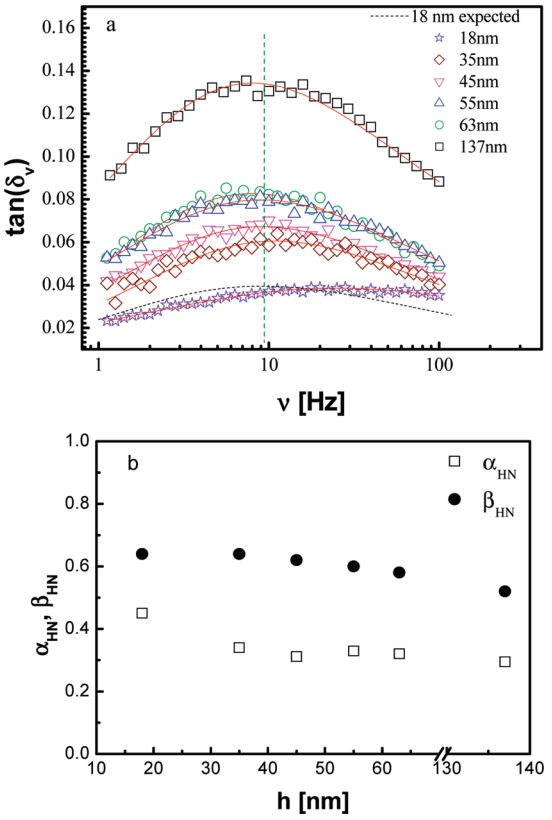

Figure 3. (a) Phase shift spectra on films with different thicknesses: 18 nm (stars), 35 nm (diamonds), 45 nm (down triangles), 55 nm (up triangles), 63 nm (circles), and 137 nm (squares) at the temperature of 324.6 K. Lines represent the fitting with eqs 3, 6, and 8. Dashed line represents the spectrum of the 18 nm film calculated by eqs 3 and 6 with the dielectric parameters obtained from the fit of the 137 thick film. (b) Shape parameters obtained from the fitting data as a function of film thickness: α_{HN} (open squares) and β_{HN} (full circles).

of 18 and 137 nm is shown in Figures 2a and 2b, respectively. A measurement below T_g is reported in Figure 2a to show the background of the instrument. Even at this low temperature and low signal the measured spectrum is correctly reflecting the presence of the high-frequency tail of the structural peak. The measured spectra above the glass transition show the presence of a relaxation peak that moves toward higher frequencies as the temperature is increased. This behavior is qualitatively the same as for dielectric spectra that can be obtained by standard dielectric relaxation spectroscopy on PVAc films.[6,7] In our analysis we described the dielectric properties of the material by the Havriliak−Negami relation:

$$\varepsilon(\omega) = \varepsilon_\infty + \frac{\Delta\varepsilon}{[1 + (i\omega\tau_{HN})^{1-\alpha_{HN}}]^{\beta_{HN}}} \quad (8)$$

where $\Delta\varepsilon$, τ_{HN}, β_{HN}, and α_{HN} are the strength, characteristic time, and shape parameters of the relaxation process. We expressed tan δ_ν in terms of eqs 3, 6, and 8 and performed best fitting of our data to determine such characteristic parameters. The fitting was performed with a Matlab program implemented with a Levenberg−Marquardt minimization routine.

In the analysis we fixed ε_∞ as constant as that known for bulk sample (ε_∞= 3.2), while the other parameters in eq 8 were adjusted to get the best fits. As shown in Figure 2a and 2b, fitting

dx.doi.org/10.1021/ma200440z |Macromolecules 2011, 44, 6588–6593

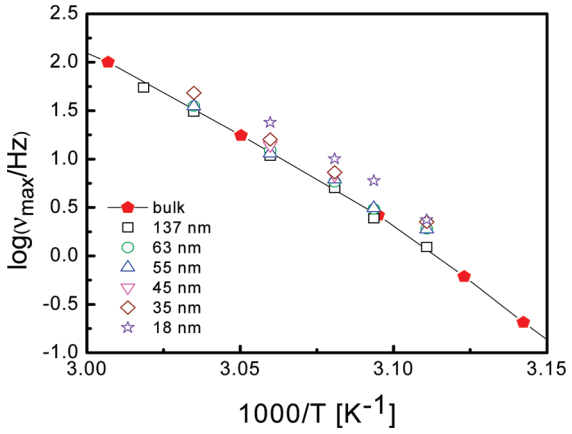

Figure 4. Logarithm of maximum frequency of dielectric loss spectra of thin films as a function of inverse temperature in comparison with data in bulk (adapted from ref 26): 18 nm (stars), 35 nm (diamonds), 45 nm (down triangles), 55 nm (up triangles), 63 nm (circles), 137 nm (squares), bulk sample (pentagon lines).

curves interpolate well the experimental data. In addition, from the fitting results the dielectric loss-tangent spectra, $\tan\delta = \varepsilon''(\omega)/\varepsilon'(\omega)$, can be carried out from eq 8 for each temperature (Figure 2c). It can be seen that the dielectric peak due to the α-relaxation process of the PVAc film shifts to higher frequency with increasing temperature, as commonly observed.

Confinement effects on dielectric relaxation were studied by measuring phase shift spectra of PVAc films with different values of thickness. Spectra measured at the temperature of 324.6 K on PVAc films of thickness down to 18 nm are presented in Figure 3a. No shift in the maximum frequency of structural relaxation process can be observed down to film thickness of 45 nm, but a shift of the peak to higher frequency comparing to the thicker films is observed at 35 nm, with a further increase for thinner films. The expected $\tan\delta_\nu$ signal at 18 nm has been calculated according to eqs 3, 6 and 8 using the dielectric permittivity estimated for the thickest film, and it is shown also in Figure 3a. The comparison with the measured signal makes clear the effect of confinement on dynamics.

A more quantitative investigation was performed by measuring and analyzing phase shift spectra at different temperatures and thickness values. Figure 4 shows the temperature dependence of the logarithm of maximum frequency. Literature data relative to a bulk sample with a similar molecular weight are also reported for comparison.[26] We found that the relaxation frequency of thin films down to thickness of around 45 nm matches that of the 137 nm film and also the bulk sample, then becoming faster for thinner films. The observed behavior here is supported by theoretical models[27,28] and many experimental results, reviewed elsewhere,[10,29] in which a significant decrease of T_g or increase of dynamic relaxation rate of thin polymer films can be observed for film thickness of the order of $2R_g$ of the polymer chains. In our measurement, for instance, we observed that the relaxation rate of films thicker than 35 nm is similar to that of the thickest film, becoming faster by about a factor of about 2 (for all investigated temperatures) when film thickness is decreased down to 18 nm, comparable to twice the gyration radius of our polymer chains.

Furthermore, we found that the shape of the structural peak is affected by confinement in ultrathin PVAc films in the same range of thickness (Figure 3b). In fact, it is observed that β_{HN} and α_{HN} both slightly increase with decreasing film thickness. This means that relaxation spectra become broader and more symmetric when film thickness decreases. Previous investigations by dielectric spectroscopy of PVAc of similar M_w than in our study showed the same behavior on capped films,[6] whereas broadness changes were not observed with the air-gap capacitor.[4] Instead in ref 7 some of the authors of ref 4 reported that PVAc capped between Al electrodes shows a variation of the relaxation time distribution, i.e., a variation of the broadness of the structural peak due to the asymmetric suppression of the slow modes. This comparison can suggest that differences in the interactions with the substrate and the "upper" electrode (if any) can be at the origin of the different observation related with the variation of broadness of the structural peak with thickness.

An enhancement of the relaxation frequency by almost 1 decade at about 20 K above T_g (which is in the range of temperature here investigated), with decreasing film thickness was found in capped films.[6,7] Such difference is observed at larger values of thicknesses in ref 6, but it is probably due to an incorrect calculation of the thickness as pointed out in ref 7. On the contrary, in the case of the free upper surface[4] no shifts of dielectric loss spectra were observed when the film thickness decreased down to 9 nm. As shown in Figure 4, an increase of relaxation rate with decreasing film thickness was observed in our study, but the increase is much smaller (by a factor of about 2) than that measured in ref 6. Since the molecular weights, and consequently R_g values, of PVAc samples are similar, effects of geometrical confinement on chain conformation cannot originate such differences. One possible explanation of the observed differences is the influence of substrates due to different interfacial interaction of substrate material with PVAc. In capped films,[6] the significant increase of molecular mobility can be caused by interfacial effects of two Al electrodes with the polymer films. When the film is in contact with only one electrode, Au in our measurements or Si in the air-gap case[4] reduced interfacial effects with the substrate on the dynamics of the thin film may be present. Moreover, the different metals used in the three investigations can have different interfacial interactions with the polymer, thus originating different effects. Another possible cause of the discrepancy with ref 4 can be found in the different condition of annealing used during film preparation (much more severe in ref 4). An interplay of the effects of interfacial interactions and annealing conditions has been recently evidenced in ref 32 where the authors point out how the chain conformation of polymer macromolecules at the interface with the substrate can assume metastable states with a lifetime much longer than the reptation time of the polymer. The lifetime and the possibility to change these metastable conformations can be related with the interfacial interactions and the temperature at which the sample is treated.

In recent publications, Serghei et al.[2] and Kim et al.[30] have suggested that the annealing and measurement conditions could be the main factor leading to the observation of altered glassy dynamics in thin polymer films. In particular, PVAc could absorb sufficient levels of water in ambient conditions, and in wet ultrathin PVAc the confinement effects are reduced or even eliminated, and wet ultrathin films showed a higher T_g in comparison with dry ones.[30] So the presence of humidity could be in principle another reason at the basis of the found discrepancy. However, we repute that humidity is not the principal cause of the observed deviation of dynamics in ultrathin films. Several reasons support this conclusion. In fact, all the samples are investigated in

the same low humidity conditions (3−5%), and consequently the relative amount of absorbed water should be the same in all the films for all thicknesses. Moreover, previous investigations report that in wet ultrathin PVAc the confinement effects are reduced or even eliminated,[30] which should lead to no change in T_g with thickness reduction. Finally, the value of T_g estimated by the data of Heinrich,[26] which well compare with our data of thicker films, is about 309 K, which is the value of T_g of dry PVAc.[31]

It can be suggested that humidity influences more the dynamics of a tiny layer of the film at the air interface, and this effect is more evident for the thinner film with respect to the thicker ones. However, we believe that such effect should be present only if a force is sustaining at the equilibrium condition (as in our experiment) a gradient of concentration of absorbed water. To our knowledge, no reasons are supporting the existence of such force in our sample, at the interface with air. Moreover, preliminary measurements at different values of relative humidity from 3 to 40% evidence the same relative variation of relaxation frequency in 21 and 128 nm thick films (data not shown). In case the humidity effect is more effective in thinner films also the effect of changing humidity should be larger in those films. Finally, using LDS technique, the topography image of the surface was always obtained before each dielectric measurement, showing stable morphology of the surface, therefore excluding the occurrence of dewetting effects.

PVAc with the same molecular weight and the same substrate material here considered was previously studied by LDS under ultrahigh vacuum with a film with thickness of 1 μm.[20] Relaxation dynamics at 320 K was observed to be about 1 decade faster compared to the bulk, along with a 4 K reduction in T_g. These results were explained by assuming that the thin layer of about 20 nm on the top of 1 μm thick polymer film is mainly probed by LDS. However, our LDS measurements on the thickest film (about 140 nm) show consistency with the data of the bulk. Such result suggests that the LDS technique can be used to probe the whole film thickness as thick as 140 nm. A deeper investigation of this aspect is presently object of our activity.

4. CONCLUSIONS

Local dielectric relaxation spectroscopy on ultrathin PVAc films with a free upper surface was performed in controlled atmosphere as a function of temperature with an AFM operated in FM-EFM mode. Phase shift spectra were measured to investigate confinement effects due to reduced thickness on the structural relaxation process. A faster relaxation was observed starting from a film thickness of 35 nm that is about 3 times the gyration radius of polymer chains, becoming even faster for thinner films. On the thinnest film of 18 nm, an increase by a factor of 2 in relaxation rate compared to the thickest ones was detected. This conclusion is based on a relative comparison of dynamics change from films with thicknesses from above to below 100 nm, and it is not dependent on the model used to analyze LDS data. The quantitative comparison with the bulk (measurements performed with standard impedance techniques) can be slightly affected by the model used in the analysis of LDS data. Such increase is smaller than that observed for PVAc films measured by previous dielectric measurements performed on capped films, but larger than that observed with air-gap capacitor. Effects due to sample preparation were avoided by careful annealing procedure. The role of the metal substrate will be investigated in further detail to rationalize the observed discrepancies.

AUTHOR INFORMATION

Corresponding Author
*E-mail: prevosto@df.unipi.it.

ACKNOWLEDGMENT

This research work has been performed in the framework of the research activity "Interface and confinement effects on physico-chemical properties of structured and composite materials" of CNR-IPCF. We thank P. Pingue (NEST-CNR and SNS) for sample deposition facilities and M. Bianucci for technical support.

REFERENCES

(1) Haick, H.; Niitsoo, O.; Ghabboun, J.; Cahen, D. *J. Phys. Chem. C* **2007**, *111*, 2318–2329.
(2) Serghei, A.; Kremer, F. *Macromol. Chem. Phys.* **2008**, *209*, 810.
(3) Sharp, J. S.; Forrest, J. A. *Phys. Rev. E* **2003**, *67*, 031805.
(4) Serghei, A.; Huth, H.; Schick, C.; Kremer, F. *Macromolecules* **2008**, *41*, 3636–3639.
(5) Erber, M.; Tress, M.; Mapesa, E. U.; Serghei, A.; Eichhorn, K. J.; Voit, B.; Kremer, F. *Macromolecules* **2010**, *43*, 7729–7733.
(6) Fukao, K.; Uno, S.; Miyamoto, Y.; Hoshino, A.; Miyaji, H. *Phys. Rev. E* **2001**, *64*, 051807.
(7) Serghei, A.; Tress, M.; Kremer, F. *Macromolecules* **2006**, *39*, 9385–9387.
(8) Wübbenhorst, M.; Murray, C. A.; Forrest, J. A.; Dutcher, J. R. *Eur. Phys. J. E* **2003**, *12*, 025.
(9) Napolitano, S.; Prevosto, D.; Lucchesi, M.; Pingue, P.; D'Acunto, M.; Rolla, P. *Langmuir* **2007**, *23*, 2103–2109.
(10) Roth, C. B.; Dutcher, J. R. *J. Electroanal. Chem.* **2005**, *584*, 13.
(11) Martin, Y.; Abraham, D. W.; Wickramasinghe, H. K. *Appl. Phys. Lett.* **1988**, *52*, 1103.
(12) Krayev, A. V.; Talroze, R. V. *Polymer* **2004**, *45*, 8195.
(13) Krayev, A. V.; Shandryuk, G. A.; Grigorov, L. N.; Talroze, R. V. *Macromol. Chem. Phys.* **2006**, *207*, 966.
(14) Sacha, G. M.; Sahagun, E.; Saenz, J. J. *J. Appl. Phys.* **2007**, *101*, 024310.
(15) Riedel, C.; Arinero, R.; Tordjeman, P.; Ramonda, M.; Lévêque, G.; Schwartz, G. A.; de Oteya, D. G.; Alegría, A.; Colmenero, J. *J. Appl. Phys.* **2009**, *106*, 024315.
(16) Fumagalli, L.; Ferrari, G.; Sampietro, M.; Gomila, G. *Appl. Phys. Lett.* **2007**, *91*, 243110.
(17) Fumagalli, L.; Ferrari, G.; Sampietro, M.; Gomila, G. *Nano Lett.* **2009**, *9*, 1604.
(18) Riedel, C.; Arinero, R.; Tordjeman, Ph.; Ramonda, M.; Lévêque, G.; Schwartz, G. A.; de Oteyza, D. G.; Alegria, A.; Colmenero, J. *Eur. Phys. J. Appl. Phys.* **2010**, *106*, 024315.
(19) Riedel, C.; Sweeney, R.; Israeloff, N. E.; Arinero, R.; Schwartz, G. A.; Alegría, A.; Tordjeman, P.; Colmenero, J. *Appl. Phys. Lett.* **2010**, *96*, 213110.
(20) Labardi, M.; Prevosto, D.; Nguyen, K. H.; Capaccioli, S.; Lucchesi, M.; Rolla, P. *J. Vac. Sci. Technol. B* **2010**, *28*, C4D11.
(21) Crider, P. S.; Majewski, M. R.; Zhang, J.; Oukris, H.; Israeloff, N. E. *Appl. Phys. Lett.* **2007**, *91*, 013102.
(22) Albrecht, T. R.; Grutter, P.; Horne, D.; Rugar, D. *J. Appl. Phys.* **1991**, *69*, 15.
(23) Glatzel, Th.; Sadewasser, S.; Lux-Steiner, M. Ch. *Appl. Surf. Sci.* **2003**, *210*, 84.
(24) Qiu, X. H.; Qi, G. C.; Yang, Y. L.; Wang, C. *J. Solid State Chem.* **2008**, *181*, 1670.
(25) Allison, S. W.; Gillies, G. T. *Rev. Sci. Instrum.* **1997**, *68*, 2615.
(26) Heinrich, W.; Stoll, B. *Prog. Colloid Polym. Sci.* **1988**, *78*, 37–53.
(27) de Gennes, P. G. *Eur. Phys. J. E* **2000**, *2*, 201.
(28) Ngai, K. L. *Eur. Phys. J. E* **2002**, *8*, 225.

(29) Alcoutlabi, M.; McKenna, G. B. *J. Phys.: Condens. Matter* **2005**, *17*, R461.
(30) Kim, S.; Mundra, M. K.; Roth, C. B.; Torkelson, J. M. *Macromolecules* **2010**, *43*, 5158–5161.
(31) Lindemann, M. K. In *Polymer Handbook*, 4th ed.; Brandrup, J., Immergut, E. H., Grulke, E. A., Eds.; John Wiley & Sons: New York, 1999; Vol. V, p 78.
(32) Napolitano, S.; Wübbenhorst, M. *Nature Commun.* **2011**, *2*, 260.